Noninvasive ^{64}Cu-ATSM and PET/CT Assessment of Hypoxia in Rat Skeletal Muscles and Tendons During Muscle Contractions

Dorthe Skovgaard[1–3], Michael Kjaer[1], Jacob Madsen[3], and Andreas Kjaer[2,3]

[1]*Institute of Sports Medicine, Bispebjerg Hospital and Faculty of Health Sciences, University of Copenhagen, Copenhagen, Denmark;* [2]*Cluster for Molecular Imaging, Faculty of Health Sciences, University of Copenhagen, Copenhagen, Denmark; and* [3]*Department of Clinical Physiology, Nuclear Medicine and PET, Rigshospitalet, Copenhagen, Denmark*

The purpose of the present study was to investigate exercise-related changes in oxygenation in rat skeletal muscles and tendons noninvasively with PET/CT and the hypoxia-selective tracer ^{64}Cu-diacetyl *bis*(N^4-methylthiosemicarbazone) (ATSM) and to quantitatively study concomitant changes in gene expression of 2 hypoxia-related genes, hypoxia-inducible factor 1α (HIF1α) and carbonic anhydrase III (CAIII). **Methods:** Two groups of Wistar rats performed 1-leg contractions of the calf muscle by electrostimulation of the sciatic nerve. After 10 min of muscle contractions, ^{64}Cu-ATSM was injected and contractions were continued for 20 min. PET/CT of both hind limbs was performed immediately and 1 h after the contractions. The exercise group (n = 8) performed only muscle contractions as described, whereas the other group, exercise plus cuff (n = 8), in addition underwent cuff-induced hypoxia during the first PET/CT scan. Standardized uptake values (SUVs) were calculated for the Achilles tendons and triceps surae muscles and were correlated to gene expression of HIF1α and CAIII using real-time polymerase chain reaction. **Results:** Immediately after the contractions, uptake of ^{64}Cu-ATSM was significantly increased, by approximately 1.5-fold in muscles and 1.3-fold in tendons, compared with resting conditions. The significant increase was maintained in late PET scans in stimulated muscles and tendons independently of cuff application. In muscles, SUV correlated significantly with gene expression of HIF1α and CAIII, whereas this coherence was not found in tendons. **Conclusion:** We found enhanced uptake of ^{64}Cu-ATSM in both early and late PET scans, thereby supporting the possibility that ^{64}Cu-ATSM registers exercise-induced transient hypoxia in both skeletal muscles and force-transmitting tendons. The fact that skeletal muscles but not tendons showed upregulation of HIF1α and CAIII could indicate that healthy tendons are less responsive than skeletal muscles to low levels of oxygen.

Received Jan. 15, 2009; revision accepted Feb. 27, 2009.
For correspondence or reprints contact: Dorthe Skovgaard, Institute of Sports Medicine, Bispebjerg Hospital, Bispebjerg Bakke 23, Copenhagen, Denmark, DK-2400.
E-mail: dskovgaard@dadlnet.dk

Key Words: hypoxia; ^{64}Cu-ATSM; tendon; skeletal muscle; exercise

J Nucl Med 2009; 50:950–958
DOI: 10.2967/jnumed.109.062216

At the onset of exercise, intracellular oxygen decreases substantially in the contracting skeletal muscles. This decrease is believed to induce immediate changes at the systemic and local levels and to constitute a main signal for more long-term muscular adjustments to exercise, such as increased skeletal muscle angiogenesis (*1,2*). It is unclear whether the force-transmitting tendons exhibit a similar decrease in intracellular oxygen during loading and to what extent any decrease would affect the adaptive mechanisms of the connective tissue.

It has been suggested that hypoxia plays a role in the development of tendon overuse injuries, in which a decreased blood flow simultaneous with an increased activity in tendons results in local tissue hypoxia, impaired nutrition, and energy metabolism (*3*). In support of this suggestion have been histologic examinations of specimens removed during surgery for tendinopathy and showing hypoxic degeneration (*4*). Furthermore, painful Achilles tendinopathy frequently develops in the relatively hypovascular anatomic region of the tendon (*5*). Also supporting hypoxia as one of the causes of tendinopathy is the finding, with microdialysis techniques, that Achilles tendinopathy clinically exhibits higher levels of lactate than are found in normal tendons, possibly indicating anaerobic metabolism (*6*).

Several attempts have been made to measure ligament and tendon oxygenation using both invasive procedures (during surgery with polarographic oxygen sensors (*7*)) and noninvasive methods (near-infrared spectroscopy [NIRS] and red-laser-light–based spectrophotometry) (*8–11*). With regard to changes in oxygenation of the tendinous structures during

loading, the use of these light-based methods has revealed conflicting results showing both a decrease (*12*) and an increase (*8*) in tendon oxygen saturation during loading.

To address this issue, exercise-related hypoxia in tendons and skeletal muscles was investigated with PET and a tracer that accumulates only in cells subjected to low oxygen tension. Preclinical studies have shown that ^{64}Cu-diacetyl *bis*(N^4-methylthiosemicarbazone) (ATSM) is reduced and retained in hypoxic tissues but is washed out rapidly from normoxic cells (*13*). The tracer has been used to assess changes in intracellular oxygen in both animal and human tumors (*14*) and in rat models of myocardiac ischemia (*15*), showing promising results for mapping hypoxic tissues. However, ^{64}Cu-ATSM has never been used for investigating changes in oxygen tension in skeletal muscles or tendons during muscle activity.

At the cellular level, response to hypoxia is complex and characterized by alterations in the expression of numerous genes, including the important hypoxia-inducible factor 1α (HIF1α) (*16*). HIF1α has been shown in humans (*1*) and rats (*17*) to be upregulated in skeletal muscles, at least at the protein level, after muscle contractions, possibly because of low intracellular oxygen.

Furthermore, several other factors, such as the carbonic anhydrases, are upregulated in hypoxic tissues. Carbonic anhydrases play a major role in pH regulation by converting CO_2 to bicarbonate ion and a proton (*18*). In skeletal muscles, the most ubiquitous carbonic anhydrase isoform is carbonic anhydrase III (CAIII), which accounts for as much as 8% of the noncontractile proteins (*19*). Although it has been debated whether a higher expression of CAIII truly reflects hypoxic conditions, a recent study found increased gene expression in the skeletal muscles of endurance athletes training for 6 wk under hypoxic conditions, indicating a possible role in pH regulation during hypoxia (*20*).

The aim of the present study was to investigate, noninvasively using PET/CT, uptake of the hypoxia PET tracer ^{64}Cu-ATSM in rat skeletal muscles and tendons in relationship to muscle contractions. Furthermore, expression of 2 hypoxia-related genes, HIF1α and CAIII, in tissue was used to verify hypoxic conditions, and a possible correlation between image-derived values for hypoxia and concomitant changes in expression of HIF1α and CAIII was investigated.

MATERIALS AND METHODS

^{64}Cu-ATSM Synthesis

$^{64}CuCl_2$ in 0.1N HCl was obtained from Risø DTU. H_2-ATSM was obtained from ABX GmbH. ^{64}Cu-ATSM was synthesized according to previously published procedures (*21,22*) with minor modifications. Briefly, 2 mL of glycine (200 mM) were added to 1 mL of 0.1N HCl $^{64}CuCl_2$ solution. The mixture was left at room temperature for 4 min before 20 μL of H_2-ATSM (1 mg of dimethyl sulfoxide per milliliter) were added. After an additional 4 min, 5 mL of water were added and the resulting mixture was passed onto a SepPak light column (Waters) and washed with 10 mL of water. The product was eluted with 1.2 mL of 50% ethanol and diluted with 9 mL of saline. Radiochemical purity (>98%) was determined with high-performance liquid chromatography. Ethanol content (approximately 5%) was determined with gas chromatography.

Experimental Protocol

The study was approved by the Animal Research Committee of the Danish Ministry of Justice. Male Wistar rats (389 g ± 15 g) were obtained from Charles River. The rats were housed in pairs and fed chow and water ad libitum. The animal room was maintained at 21°C with a 12-h:12-h light:dark cycle. General anesthesia was induced with a subcutaneous injection of fluanisone/fentanyl citrate and midazolam (5 mg/0.625 mL/kg) and was maintained during the experiment by repeated administrations of the same anesthetic (2.5 mg/0.313 mL/kg) every 20 min. The rats performed 1-leg contractions of the calf muscles by electrostimulation of the sciatic nerve. The contralateral leg served as the resting control. The necessary surgical procedure has recently been described in detail and has proven suitable for detecting metabolic changes in tendons and skeletal muscles with PET/CT (*23*). After 10 min of muscle contractions, ^{64}Cu-ATSM (21.9 ± 1.27 MBq) was injected as a bolus through a tail vein catheter (Neoflon, 24-gauge; BD) and contractions were continued for another 20 min.

The specific protocol (Supplemental Fig. 1; supplemental materials are available online only at http://jnm.snmjournals.org) was designed both to test changes in the uptake of ^{64}Cu-ATSM in muscles and tendons after contractions and to test for irreversible trapping of ^{64}Cu-ATSM. The rats were divided into 2 groups, an exercise group (E group) (n = 8) and an exercise-plus-cuff group (EC group) (n = 8). In both groups, the rats were placed prone on the acquisition bed immediately on cessation of muscle contractions, and an early PET scan was performed with the 2 hind limbs in the field of view. Afterward, a CT scan for anatomic information and a late PET scan (60 min after contractions) were acquired. The EC group was included to investigate the irreversibility of ^{64}Cu-ATSM uptake by preventing reperfusion of the exercised hind limb with a tight elastic femoral band aimed at maintaining a hypoxic environment in the studied tissues. The band was applied at the last muscle contraction and was kept tight during the first early PET scan, after which it was removed, allowing reestablishment of blood flow to the exercised leg between the early and late PET scans. In both groups, the animals were sacrificed immediately after the last PET scan, and both the Achilles tendons and the soleus muscles were carefully removed and placed in RN*Alater* (Ambion Inc.) for subsequent analysis of gene expression of the 2 hypoxia-related molecules (HIF1α and CAIII).

Image Acquisition and Processing

CT data were acquired with a MicroCAT II Tomograph (Siemens Medical Solutions). The x-ray tube was set at 40 kVp and had a 0.5-mm plate of added aluminum filtration. The exposure time was 700 ms per projection, and the tube current was 500 μA. A total of 800 projections was used for a full 360° scan. Images were reconstructed using the Sheep–Logan algorithm. These settings have earlier been shown to provide the best image quality for soft tissues (*23*).

A 30-min static emission scan was acquired with a microPET Focus 220 (Siemens Medical Solutions). The late PET scan was followed by a 6-min transmission scan with a ^{57}Co pin source. All list-mode data were sorted into 3-dimensional sinograms using a span of 3 and a ring difference of 47. Images were reconstructed

using 2-dimensional ordered-subset expectation maximization. In addition to attenuation, the emission data were corrected for scatter, dead time, and decay time.

^{64}Cu-ATSM uptake in the Achilles tendon and the triceps surae muscle (covering both gastrocnemius and soleus) was quantitated (Bq/cm^3) from each animal using the image analysis software Inveon (Siemens Medical Solutions). The software allows for fusion of the PET images with CT for anatomic information. The 2 image modalities were aligned on the basis of 3 distinctive fiducial markers placed directly on the animal bed within the field of view although not near the regions of interest (≥5 mm). The 3-dimensional regions of interest were drawn on the CT image so as to cover the Achilles tendon and the midportion of the triceps surae muscle including both (red and white) gastrocnemius and soleus. During subsequent analysis, standardized uptake values (SUVs) in the individual regions of interest were calculated by dividing the mean specific activity by injected dose and animal weight, assuming 1 cm^3 = 1 g.

Gene Expression

Immediately after the second PET scan, the animals were sacrificed by decapitation. Rapidly, both Achilles tendons and soleus muscles were removed and placed in RN*Alater* for subsequent analyses. Samples were kept in RN*Alater* overnight, after which RN*Alater* was removed and the samples were stored at −80°C for later use.

Total RNA from all tissue types was extracted according to the method described by Chomczynski and Sacchi (*24*). All samples were weighed before RNA extraction. In brief: tissue samples were homogenized in TRI Reagent (Molecular Research Center, Inc.) using a Bertin Precellys 24 (Bertin Technologies) homogenizer, ceramic beads (CK 28; Bertin Technologies), and a protocol consisting of 6,000*g* for 20 s repeated 5 times or until all visible tissue was dissolved.

After homogenization, 1-bromo-3-chloropropane (Molecular Research Center, Inc.) was added (100 μL per 1,000 μL of TRI Reagent) to separate the samples into an aqueous and an organic phase. After isolation of the aqueous phase, RNA was precipitated using isopropanol. The RNA pellet was then washed in ethanol and subsequently dissolved in RNase-free water. RNA integrities and concentrations were determined by Bio-analyzer 2100 (Agilent Technologies). Subsequently, 2 μg of total RNA from muscles and 500 ng from tendons were reverse-transcribed using StrataScript QPCR cDNA Synthesis Kit (Stratagene).

HIF1α and CAIII were quantified by real-time polymerase chain reaction based on TaqMan chemistry. Amplification was performed on a MX3000P apparatus (Stratagene) as a triplex with HIF1α and CAIII as genes of interest and TBP and RPL13 as housekeeping genes for muscles and tendons, respectively. The testing and selection of these housekeeping genes have previously been described in detail (*23*). Real-time polymerase chain reaction primers and probes for all genes measured were designed and tested for secondary structures as well as homology using Beacon Designer software (Biosoft). All oligonucleotides were purchased from Sigma-Aldrich (Table 1). The optimal primer and probe concentration were determined beforehand. Standard curves with freshly made 5-fold dilutions were always included in the experiments to enable efficiency corrections in the calculation of the relative expression level. Expression of the genes of interest was quantified for each animal using the ΔΔCt method with the relevant housekeeping gene as the normalizer gene and control values from each paired (resting) leg as the calibrator.

Statistical Analysis

t testing for paired samples was used to compare the SUV of ^{64}Cu-ATSM between resting and loaded tendons and muscles between the 2 groups (E and EC). For comparison of SUV between the E and the EC group, *t* testing for unpaired samples was used. Furthermore, the association between tendon and muscle SUVs in the early and late scans was also analyzed using linear regression, in the 2 groups. Expressions of the 2 genes of interest, HIF1 and CAIII, were log-transformed before analysis to obtain the normal distribution and compared within each group (rest vs. exercise) using a *t* test for paired samples. Lastly, the dependency between SUV and the gene expression of HIF1α and CAIII in each group was compared using linear regression. A *P* level of 0.05 was considered significant. The results are expressed as mean ± SEM except for the changes in gene expression, which are presented as geometric mean ± SEM.

RESULTS

Uptake of ^{64}Cu-ATSM in Muscles and Tendons

Representative corresponding coronal CT and PET images are shown in Figure 1. Uptake of ^{64}Cu-ATSM was assessed in the Achilles tendon and triceps surae muscle immediately after contractions and 1 h after contractions. In the E group immediately after contractions, uptake of ^{64}Cu-ATSM was significantly higher in contracted muscles than in resting muscles. The increase was approximately 1.5-fold (0.59 ± 0.03 vs. 0.38 ± 0.03, $P = 0.0002$) (Fig. 2A). Uptake was also significantly higher in force-transmitting tendons than in resting tendons. The increase was approximately 1.3-fold (0.72 ± 0.04 vs. 0.56 ± 0.05, $P = 0.006$) (Fig. 2B). A significant difference between the stimulated and the resting legs was maintained on late PET scans for

TABLE 1. Primer and Probe Sequences and Amplicon Length for Investigated Genes

Gene	Forward primer (5′-3′)	Reverse primer (5′-3′)	5′ fluorophore	Probe (5′-3′)	3′ quencher	Amplicon length
TBP	tccttcaccaatgactcctatgac	tcaagtttacagccaagattcacg	HEX	cctgccacaccagcctctgagagc	BHQ-1	120 bp
RPL13	tcgtgaggtgccctacagttag	ggtgcgtgccattttcttgtg	HEX	cacaccaaggtccgggctggcag	BHQ-1	107 bp
Muscle HIF1α	ggattccagcagacccagttac	gggtagaaggtggagatgaatc	FAM	accatcactgtcactgccaccgca	BHQ-1	139 bp
Tendon HIF1α	caagcagcaggaattggaacg	tgctccattccatcctgttcac	FAM	tgcagcaaccaggtgaccgtgcc	BHQ-1	116 bp
Muscle CAIII	aggctccttttaatcacttcgac	ctttcagtagcagccacacaatg	CY5	cgtgcctgttccctgcttgccgg	BHQ-2	123 bp
Tendon CAIII	gaggctctccttttaatcacttcga	tcactgtcatgggctctttcag	CY5	acaatgcactcctcgcagggtggc	BHQ-2	139 bp

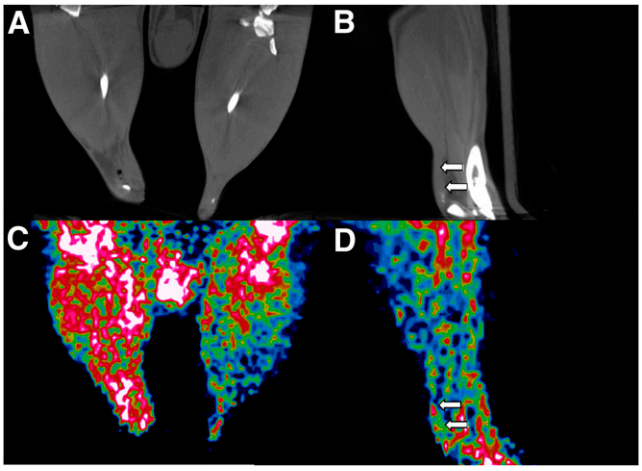

FIGURE 1. Representative CT and PET images of hind limbs of rat immediately after unilateral electrostimulated muscle contractions. (A and C) Corresponding CT and PET images (coronal) showing clearly higher uptake of ^{64}Cu-ATSM on stimulated left side. (C and D) Corresponding CT and PET images (sagittal) of right hind limb. Arrows mark clearly distinctive Achilles tendon.

both muscles (0.53 ± 0.04 vs. 0.34 ± 0.04, $P = 0.002$) (Fig. 2A) and tendons (0.70 ± 0.04 vs. 0.56 ± 0.05, $P = 0.04$) (Fig. 2B). No significant decrease was found when uptake of ^{64}Cu-ATSM in resting tendons and stimulated tendons was compared between the early and late scans. Linear regression analyses revealed a good correlation between the early and late PET scans for tendons (resting tendons, $R^2 = 0.87$, $P < 0.001$; loaded tendons, $R^2 = 0.88$, $P < 0.001$). In contrast, there was a small (~10%) washout of the tracer from both stimulated and resting skeletal muscles. Importantly, the SUVs at the 2 time points still correlated significantly (resting muscles, $R^2 = 0.56$, $P < 0.05$; exercised muscles, $R^2 = 0.71$, $P < 0.01$).

In the EC group, in which a tight cuff was placed around the stimulated leg immediately at the end of contractions to prevent reoxygenation, uptake of ^{64}Cu-ATSM revealed a pattern similar to that of the E group, with significantly increased uptake in contracted muscles and in force-transmitting tendons, compared with resting conditions (early PET scan: 0.54 ± 0.03 for exercised muscles vs. 0.33 ± 0.01 for resting muscles, $P = 0.0002$, and 0.68 ± 0.05 for loaded tendons vs. 0.57 ± 0.05 for resting tendons, $P = 0.006$) (Figs. 2C and 2D). Furthermore, application of the cuff during the first PET scan did not increase uptake of ^{64}Cu-ATSM in tendons, and SUV was also unchanged on the late scan (late PET scan: 0.48 ± 0.08 for exercised muscles vs. 0.30 ± 0.01 for resting muscles, $P = 0.0002$, and 0.70 ± 0.05 for loaded tendons vs. 0.56 ± 0.04 for resting tendons, $P = 0.02$) (Figs. 2C and 2D). For skeletal muscles, the same picture as in the E group was apparent in the EC group, with increased uptake in the stimulated leg and parallel washout of the tracer from both rested and stimulated–cuffed leg on a magnitude of 10%. Likewise, the correlation between SUV at early and late time points was significant for both muscles (resting, $R^2 = 0.92$, $P < 0.01$; exercised, $R^2 = 0.64$, $P < 0.05$) and tendons (resting, $R^2 = 0.69$, $P < 0.05$; exercised, $R^2 = 0.91$, $P < 0.001$).

Gene Expression of HIF1α and CAIII

In muscles, HIF1α messenger RNA (mRNA) expression was significantly greater under sciatic nerve stimulation than under resting conditions in both the E group (1.16 ± 0.04 for exercised muscles vs. 0.99 ± 0.03 for resting muscles, $P = 0.04$) (Fig. 3A) and the EC group (1.17 ± 0.08 for exercised muscles vs. 0.93 ± 0.09 for resting muscles, $P = 0.003$) (Fig. 3B). In Achilles tendons, HIF1α mRNA increased significantly only in the EC group (1.36 ± 0.06 for loaded tendons vs. 0.99 ± 0.03 for resting tendons, $P = 0.004$) (Fig. 3D); in the E group, HIF1α mRNA did not change in the tendons subjected to mechanical loading (0.93 ± 0.09 for resting tendons vs. 0.94 ± 0.13 for loaded tendons, $P = 0.95$) (Fig. 3C).

In skeletal muscles, 30 min of contractile activity led to increasing CAIII mRNA levels in the E group (1.06 ± 0.01 for exercised muscles vs. 1.00 ± 0.02 for resting muscles, $P = 0.02$) but not in the EC group (1.01 ± 0.05 for exercised muscles vs. 0.96 ± 0.06 for resting muscles, $P = 0.62$). No effect on CAIII mRNA levels in Achilles tendons could be detected after contractions in either of the groups (E: 0.80 ± 0.12 for exercised muscles vs. 0.93 ± 0.10 for resting muscles, $P = 0.51$; EC: 0.95 ± 0.10 for exercised muscles vs. 1.19 ± 0.13 for resting muscles, $P = 0.35$).

Correlation Between SUV of ^{64}Cu-ATSM and Gene Expression of HIF1α and CAIII

In the E group, the SUV in skeletal muscles significantly correlated with HIF1α ($R^2 = 0.364$, $P = 0.015$) (Fig. 4A) and CAIII ($R^2 = 0.464$, $P = 0.004$) (Fig. 4B). Neither of these correlations was found in the EC group. Uptake of ^{64}Cu-ATSM in tendons did not correlate with gene expression of HIF1α and CAIII in either group E or group EC.

DISCUSSION

With the hypoxia tracer ^{64}Cu-ATSM and PET/CT, we noninvasively demonstrated that intracellular oxygen levels decrease in both muscles and force-transmitting tendons as a result of muscle contractions. The image-derived results corresponded to concomitant changes in the hypoxia-responsive genes HIF1α and CAIII in skeletal muscles and, to a lesser degree, in tendons.

Several other studies have measured oxygenation in musculoskeletal tissues during exercise using various methods (*12,25*). With ^{1}H nuclear magnetic resonance studies of deoxymyoglobin, a substantial decrease in intracellular oxygen in skeletal muscles at the onset of exercise has been demonstrated (*2*). This decrease corresponds well with the present results showing higher uptake of ^{64}Cu-ATSM in contracting skeletal muscles, implying a decrease in intracellular oxygen. However, the method of ^{1}H nuclear mag-

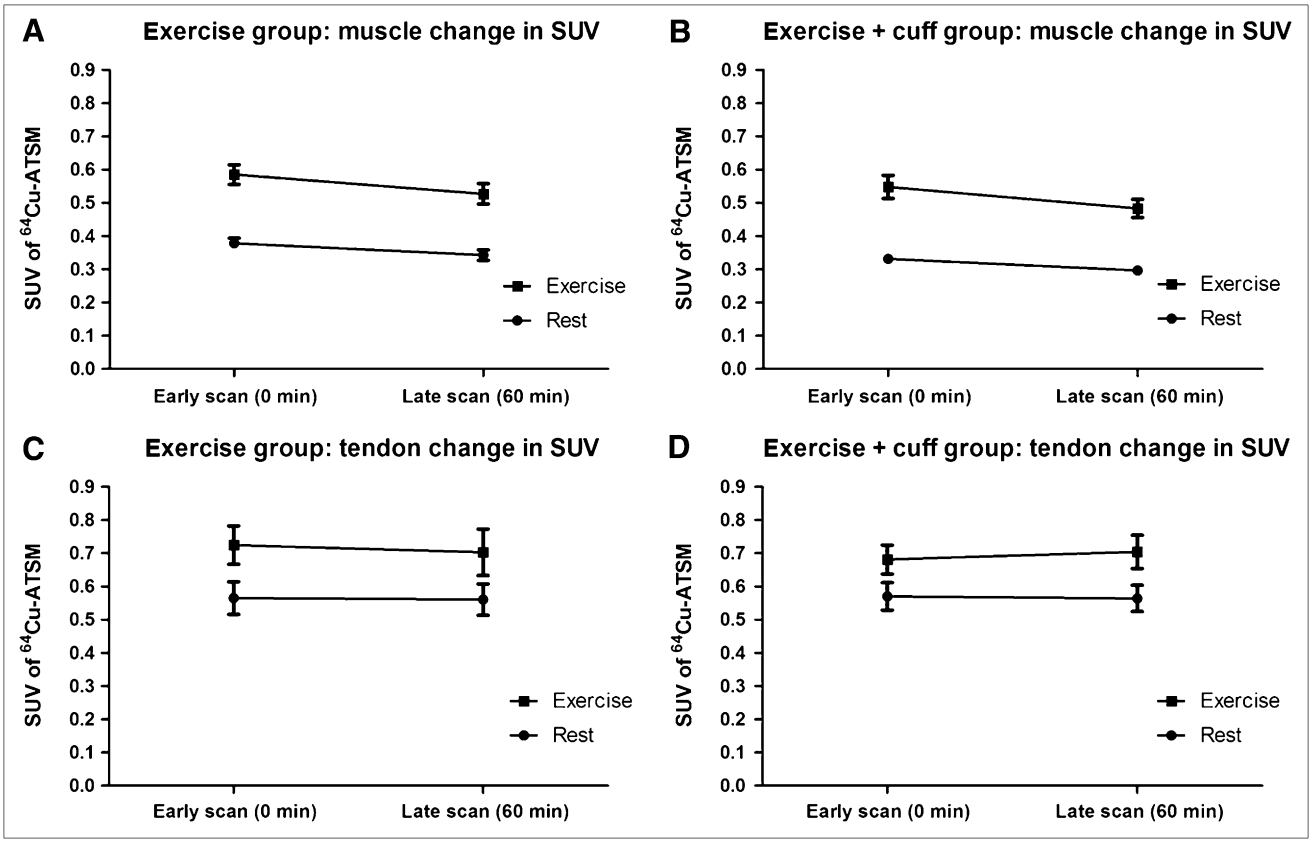

FIGURE 2. Changes in SUVs of ^{64}Cu-ATSM from early to late PET scans in muscles (A and B) and tendons (C and D) in E group and EC group. Figures display changes in SUVs from early scans (0 min after contractions) to late scans (60 min after contractions). In both groups, SUVs of ^{64}Cu-ATSM in skeletal muscles and Achilles tendons are higher in exercised hind limbs than in resting hind limbs. Furthermore, SUVs are consistently higher in tendons than in muscles in exercised and resting hind limbs. SUVs are maintained in tendons from early to late scans; however, both E group and EC group show minor (~10%, $P < 0.05$) decrease in SUV in muscles from early to late scans. Values are means, with bars representing SEM.

netic resonance spectroscopy cannot be extended to tendinous tissues, because myoglobin is specific for the contractile elements. With NIRS, a fall in oxygen saturation in the human peritendinous region of the Achilles tendon was demonstrated during muscle contractions of the calf muscles, but only at the highest workloads (7–9 W) (*12*). These results agree with the present results. However, a recent study (*8*) using red laser lights demonstrated a decrease in saturation only during a single isometric contraction, whereas repeated contractions increased oxygen saturation in the Achilles tendon and this increase was maintained during the 10-min recovery period. There is no good explanation for these contradictory results, but likely causes could be differences in the methods of estimating oxygen saturation, in the depth of measurements, and, probably, in the workload of the repetitive muscle contractions.

Furthermore, with NIRS and red laser light, the spatially resolved spectroscopy (SRS-O_2) value represents the mean saturation of the entire hemoglobin volume present in the tissue region and accounts for changes in the proportions of the hemoglobin and hemoglobin O_2 volumes. The SRS-O_2 saturation reflects predominantly the mean of arteriolar, capillary, and venular O_2 saturations and some contribution from myoglobin and, therefore, only to a certain degree reflects intracellular oxygen (*12*).

An advantage when using PET is the possibility of combining the functional PET images with anatomic information from CT images, ensuring that the position of the studied tissues is precisely known. Furthermore, assessment of hypoxia using PET gives an opportunity to study several different regions and tissues simultaneously. In contrast, near-infrared/red laser light allows the study of only superficial structures, at a depth of 3–5 mm (red laser light) to 2–3 cm (NIRS) (*26*), and the number of studied regions is limited by the number of channels in the equipment. Another advantage with PET is the possibility of estimating the heterogeneity of the studied regions. This ability could be of relevance when one is studying contracting skeletal muscles, in which the heterogeneous blood flow distribution may have a significant impact on oxygen and nutrient delivery (*27*). The heterogeneity of hypoxia might also be important in force-transmitting tendons; a nonuniform loading pattern in distinct tendinous

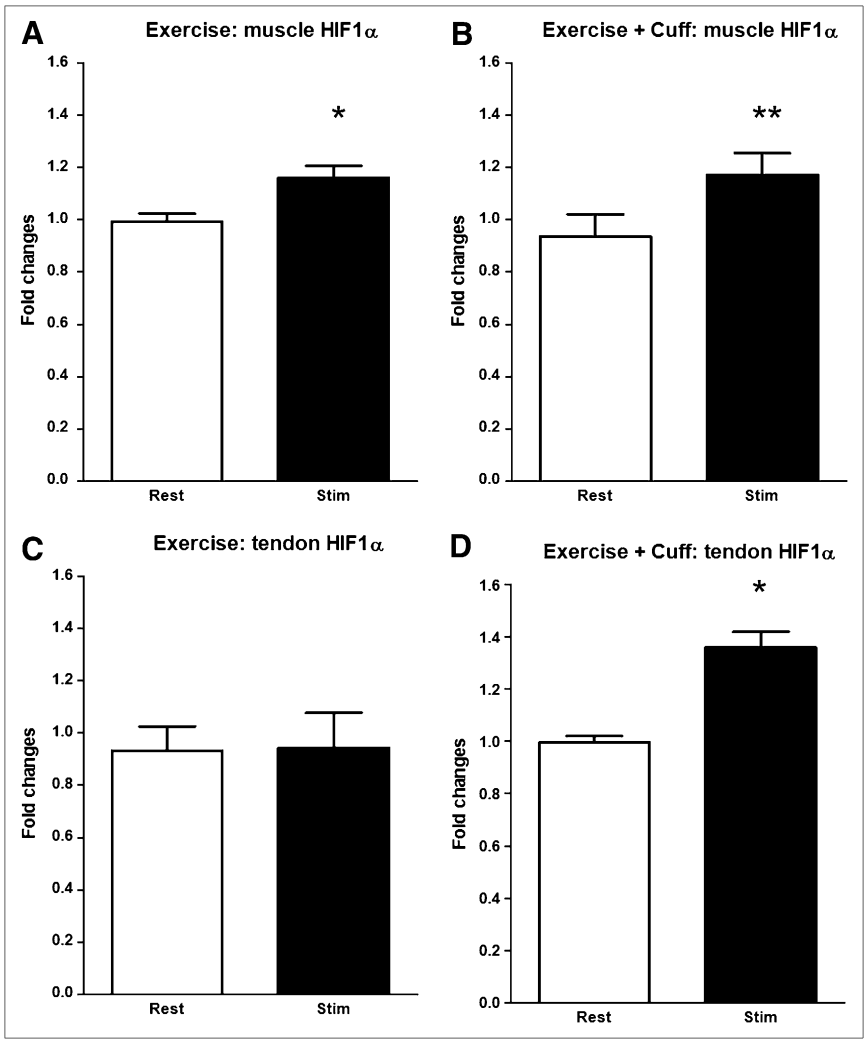

FIGURE 3. Gene expression of HIF1α in muscles (A and B) and tendons (C and D) in E group and EC group. HIF1α mRNA normalized to housekeeping genes TBP (soleus muscle) and RPL13 (Achilles tendon). Data are represented as geometric means (±SEM) of fold changes in soleus muscle and Achilles tendon subjected to isometric muscle contractions, compared with (paired) respective control samples. In skeletal muscles, HIF1α mRNA is elevated subsequent to isometric electrostimulated muscle contractions in both E group and EC group. Applied load of Achilles tendon induced by electrostimulated muscle contraction did not by itself increase HIF1α mRNA levels over resting levels. In contrast, application of cuff around contracted leg induced significant increase in HIF1α gene expression in Achilles tendon.

structures such as the Achilles tendon due to heterogeneous activation of the calf muscle has been suggested (*28*).

Importantly, the SUV of ^{64}Cu-ATSM was higher in both resting and loaded tendons than in the corresponding muscles, possibly indicating that cellular oxygenation under both resting and loaded conditions is higher for skeletal muscles than for tendon fibroblasts. This possibility corresponds to the results of a human study with NIRS that found lower oxygen saturation in the human peritendinous region than in the triceps surae muscle both during rest and during dynamic plantar-flexion exercise (*12*). At present, the significance of this phenomenon is not known.

Correlation Between ^{64}Cu-ATSM Uptake and Gene Expression

HIF1α is considered a key regulator of adaptation to low intracellular oxygen and is likely to be involved in various metabolic processes such as angiogenesis, matrix protein, and glucose metabolism (*16,17,29*). In the present study, gene expression of HIF1α was increased in skeletal muscles in response to exercise. Importantly, there was a significant correlation between the image-derived values of ^{64}Cu-ATSM uptake in skeletal muscles and HIF1α expression. This correlation supports the possibility that uptake of ^{64}Cu-ATSM in skeletal muscles indeed reflects intracellular hypoxia leading to HIF1α expression.

The pattern was less clear in the connective tissue of the Achilles tendon, in which the load applied by the muscle contractions could not alone induce changes in the gene expression of HIF1α despite decreased intracellular oxygen as indicated by the higher uptake of ^{64}Cu-ATSM. In contrast, the cuff group exhibited a significant 40% increase after muscle contractions and a prolongation of the hypoxic condition. This finding could be explained by an organ-specific selectivity in the ability of low oxygen tension to stimulate HIF1α mRNA and by the fact that tendon connective tissue is rather resistant to decreased intracellular oxygen during physiologic loading. It is possible that the adaptive mechanisms regulated by HIF1α activation are induced only when hypoxia is more apparent, either when nutritive flow to the tendons is seriously compromised, as, for example, during application of the cuff, or when the hypoxia is

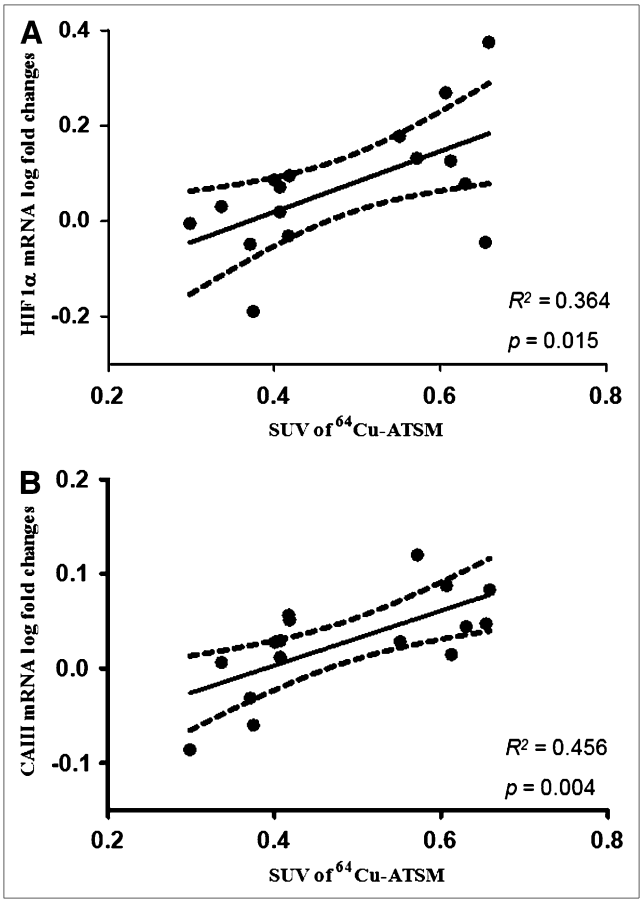

FIGURE 4. Correlation between SUV of ^{64}Cu-ATSM and gene expression of HIF1α (A) and CAIII (B) in skeletal muscles. In soleus muscle, uptake of ^{64}Cu-ATSM expressed as SUV correlated significantly with log-transformed gene expression of both CAIII and HIF1α. Correlation coefficient, *P* value, and 95% confidence limits are shown.

temporarily prolonged for more than 30 min. Several in vitro studies have supported the notion that tenocytes are more resistant to hypoxia than are other cell types; for example, compared with similar cell types, tendon cells subjected to anoxia exhibit less apoptosis (*30*) and are less affected by the production of matrix components, including collagen (*31*) and continuous cellular proliferation (*32*).

In the present study, gene expression of CAIII was enhanced in skeletal muscles after 30 min of electrically induced muscle contractions, and CAIII expression correlated significantly with uptake of ^{64}Cu-ATSM in the E group. This correlation points toward a relationship between intracellular oxygen in the myocytes and CAIII expression, indicating that this enzyme has at least some role in myocellular oxygen homeostasis. However, the importance of CAIII in pH regulation in skeletal muscles during exercise is debated. Although some have suggested that the enhanced mRNA level of CAIII represents a transcriptional adaptation in response to the reduced intracellular pH due to the anaerobic conditions in the muscle cells (*20*), others have questioned this hypothesis (*33*).

Unlike the skeletal muscles, the Achilles tendons showed no upregulation of CAIII either during exercise or after exercise and prolonged cuff-induced hypoxia. Accordingly, no correlation could be demonstrated between the uptake of ^{64}Cu-ATSM and CAIII expression in the Achilles tendon. Therefore, contrary to our hypothesis, CAIII does not appear to have any major importance in the adaptive mechanisms to hypoxia in tendon tissue, underlining the fact that the same enzymes exhibit divergent roles in different tissues.

Methodologic Considerations

When ^{64}Cu-ATSM is used as a hypoxia tracer in various tissues during exercise, one major concern is that ^{64}Cu-ATSM PET is usually applied under experimental and clinical conditions in which the oxygen tension is thought to be constitutively low, as in hypoxic tumors (*34–36*) or in ischemic heart muscle after compromise of the coronal blood flow (*15,21*). In contrast, during exercise, low oxygen tension is present only during the contractile activity and is considered to be reversed immediately after cessation of contractions. Therefore, in this situation it is crucial that the tracer be irreversibly trapped because the postexercise PET scan will present only the trapped fraction of ^{64}Cu-ATSM. The role of reoxygenation has been studied in vitro, and a lower uptake of ^{64}Cu-ATSM has been shown after reoxygenation than after continuous hypoxia (*37*). Interestingly, the present study provides data suggesting that even 1 h after cessation of contractions, a difference still exists between the hypoxia-challenged contracted site and the control leg, possibly representing the irreversibly trapped fraction. In fact, there appeared to be no washout of the tracer from the Achilles tendon between the early and late scans and only minor washout from the muscle, in the range of 10%. Therefore, on the basis of postexercise PET scans, the tracer seems useful for studying hypoxia during exercise.

It is well established that muscle contractions lead to increased blood flow in both the contracting muscles and the force-transmitting tendons (*12,38*). An increased blood flow leads to higher delivery of the tracer, but higher delivery is not believed to contribute significantly to the increased SUV after exercise because ^{64}Cu-ATSM is retained only when intracellular oxygen is low. Some have questioned ^{64}Cu-ATSM as a universal marker of hypoxia, with data failing to demonstrate expected changes in ^{64}Cu-ATSM uptake in response to modulation of the oxygenation status of murine tumors, and it has been suggested that some hypoxia-independent mechanisms might also influence ^{64}Cu-ATSM uptake (*35,39*). However, the present study—in line with several others (*15,21*), including studies of biodistribution (*40*)—supports the rapid and selective uptake of ^{64}Cu-ATSM in hypoxic and ischemic tissue within 20 min after administration. The EC group was included to rule out a large outflow of untrapped tracer immediately at the end of exercise because of reoxygenation. Application of a tight cuff around the exercising leg immediately at the end of muscle contractions

prevented reoxygenation of the tissues. Under these circumstances, SUVs were not affected, and this result implies that ^{64}Cu-ATSM PET performed after exercise indeed reflects the development of hypoxia during exercise even 1 h into the recovery period.

CONCLUSION

The present study demonstrated, with PET methodology, an enhanced uptake of ^{64}Cu-ATSM reflecting transient hypoxia in both skeletal muscles and force-transmitting tendons during muscle contractions. The correlation between the image-derived uptake of ^{64}Cu-ATSM and the expression of the hypoxia-relevant enzymes HIF1α and CAIII in skeletal muscles points toward intracellular oxygen as a mediator of transcriptional changes in a dose–response manner. Importantly, tendons showed higher uptake of ^{64}Cu-ATSM under both resting and loaded conditions than did muscles, with no significant upregulation of the hypoxia-related genes, indicating a less pronounced cellular response, when healthy tendons were subjected to low levels of oxygen. The PET method can be extended to use on humans for investigating the development of hypoxia in several tissues simultaneously during exercise. Furthermore, the PET method can be used clinically to investigate hypoxia in skeletal muscles, such as in patients with peripheral artery disease or with myopathies such as the mitochondria-related syndromes. Finally, the PET method can be used to investigate hypoxia in patients with tendinopathy during exercise-induced loading of the diseased tendons.

ACKNOWLEDGMENTS

This work was supported by the Danish Medical Research Council, the Danish National Advanced Technology Foundation, the Novo Nordisk Foundation, the Lundbeck Foundation, and the A.P. Moeller Foundation.

REFERENCES

1. Ameln H, Gustafsson T, Sundberg CJ, et al. Physiological activation of hypoxia inducible factor-1 in human skeletal muscle. *FASEB J.* 2005;19:1009–1011.
2. Richardson RS, Duteil S, Wary C, Wray DW, Hoff J, Carlier PG. Human skeletal muscle intracellular oxygenation: the impact of ambient oxygen availability. *J Physiol.* 2006;571:415–424.
3. Pufe T, Petersen WJ, Mentlein R, Tillmann BN. The role of vasculature and angiogenesis for the pathogenesis of degenerative tendons disease. *Scand J Med Sci Sports.* 2005;15:211–222.
4. Kvist M, Jozsa L, Jarvinen MJ, Kvist H. Chronic Achilles paratenonitis in athletes: a histological and histochemical study. *Pathology.* 1987;19:1–11.
5. Fenwick SA, Hazleman BL, Riley GP. The vasculature and its role in the damaged and healing tendon. *Arthritis Res.* 2002;4:252–260.
6. Alfredson H, Bjur D, Thorsen K, Lorentzon R, Sandstrom P. High intratendinous lactate levels in painful chronic Achilles tendinosis: an investigation using microdialysis technique. *J Orthop Res.* 2002;20:934–938.
7. Stone KR, Bowman HF, Boland A, Steadman JR. Ligament and tendon oxygenation measurements using polarographic oxygen sensors. *Arthroscopy.* 1987;3:187–195.
8. Kubo K, Ikebukuro T, Tsunoda N, Kanehisa H. Noninvasive measures of blood volume and oxygen saturation of human Achilles tendon by red laser lights. *Acta Physiol (Oxf).* 2008;193:257–264.
9. Knobloch K, Schreibmueller L, Meller R, Busch KH, Spies M, Vogt PM. Superior Achilles tendon microcirculation in tendinopathy among symptomatic female versus male patients. *Am J Sports Med.* 2008;36:509–514.
10. Knobloch K, Kraemer R, Jagodzinski M, Zeichen J, Meller R, Vogt PM. Eccentric training decreases paratendon capillary blood flow and preserves paratendon oxygen saturation in chronic Achilles tendinopathy. *J Orthop Sports Phys Ther.* 2007;37:269–276.
11. Knobloch K, Kraemer R, Lichtenberg A, et al. Achilles tendon and paratendon microcirculation in midportion and insertional tendinopathy in athletes. *Am J Sports Med.* 2006;34:92–97.
12. Boushel R, Langberg H, Green S, Skovgaard D, Bulow J, Kjaer M. Blood flow and oxygenation in peritendinous tissue and calf muscle during dynamic exercise in humans. *J Physiol.* 2000;524:305–313.
13. Vavere AL, Lewis JS. Cu-ATSM: a radiopharmaceutical for the PET imaging of hypoxia. *Dalton Trans.* 2007;(43):4893–4902.
14. Burgman P, O'Donoghue JA, Lewis JS, Welch MJ, Humm JL, Ling CC. Cell line-dependent differences in uptake and retention of the hypoxia-selective nuclear imaging agent Cu-ATSM. *Nucl Med Biol.* 2005;32:623–630.
15. Lewis JS, Herrero P, Sharp TL, et al. Delineation of hypoxia in canine myocardium using PET and copper(II)-diacetyl-*bis*(N^4-methylthiosemicarbazone). *J Nucl Med.* 2002;43:1557–1569.
16. Ke Q, Costa M. Hypoxia-inducible factor-1 (HIF-1). *Mol Pharmacol.* 2006;70:1469–1480.
17. Tang K, Breen EC, Wagner H, Brutsaert TD, Gassmann M, Wagner PD. HIF and VEGF relationships in response to hypoxia and sciatic nerve stimulation in rat gastrocnemius. *Respir Physiol Neurobiol.* 2004;144:71–80.
18. Pastorekova S, Zatovicova M, Pastorek J. Cancer-associated carbonic anhydrases and their inhibition. *Curr Pharm Des.* 2008;14:685–698.
19. Zimmerman UJ, Wang P, Zhang X, Bogdanovich S, Forster R. Anti-oxidative response of carbonic anhydrase III in skeletal muscle. *IUBMB Life.* 2004;56:343–347.
20. Zoll J, Ponsot E, Dufour S, et al. Exercise training in normobaric hypoxia in endurance runners. III. Muscular adjustments of selected gene transcripts. *J Appl Physiol.* 2006;100:1258–1266.
21. Fujibayashi Y, Cutler CS, Anderson CJ, et al. Comparative studies of Cu-64-ATSM and C-11-acetate in an acute myocardial infarction model: ex vivo imaging of hypoxia in rats. *Nucl Med Biol.* 1999;26:117–121.
22. O'Donoghue JA, Zanzonico P, Pugachev A, et al. Assessment of regional tumor hypoxia using ^{18}F-fluoromisonidazole and ^{64}Cu(II)-diacetyl-bis(N4-methylthiosemicarbazone) positron emission tomography: Comparative study featuring microPET imaging, Po2 probe measurement, autoradiography, and fluorescent microscopy in the R3327-AT and FaDu rat tumor models. *Int J Radiat Oncol Biol Phys.* 2005;61:1493–1502.
23. Skovgaard D. Exercise-induced increase in glucose uptake and glucose transporter gene expression in rat skeletal muscle and tendon: use of high resolution PET/CT. *Eur J Nucl Med Mol Imaging.* In press.
24. Chomczynski P, Sacchi N. Single-step method of RNA isolation by acid guanidinium thiocyanate-phenol-chloroform extraction. *Anal Biochem.* 1987;162:156–159.
25. Soller BR, Hagan RD, Shear M, et al. Comparison of intramuscular and venous blood pH, PCO_2 and PO_2 during rhythmic handgrip exercise. *Physiol Meas.* 2007;28:639–649.
26. Boushel R, Langberg H, Olesen J, Gonzales-Alonzo J, Bulow J, Kjaer M. Monitoring tissue oxygen availability with near infrared spectroscopy (NIRS) in health and disease. *Scand J Med Sci Sports.* 2001;11:213–222.
27. Kalliokoski KK, Langberg H, Ryberg AK, et al. Nitric oxide and prostaglandins influence local skeletal muscle blood flow during exercise in humans: coupling between local substrate uptake and blood flow. *Am J Physiol Regul Integr Comp Physiol.* 2006;291:R803–R809.
28. Bojsen-Moller J, Hansen P, Aagaard P, Svantesson U, Kjaer M, Magnusson SP. Differential displacement of the human soleus and medial gastrocnemius aponeuroses during isometric plantar flexor contractions in vivo. *J Appl Physiol.* 2004;97:1908–1914.
29. Fluck M. Functional, structural and molecular plasticity of mammalian skeletal muscle in response to exercise stimuli. *J Exp Biol.* 2006;209:2239–2248.
30. Scott A, Khan KM, Duronio V. IGF-I activates PKB and prevents anoxic apoptosis in Achilles tendon cells. *J Orthop Res.* 2005;23:1219–1225.
31. Webster DF, Burry HC. The effects of hypoxia on human skin, lung and tendon cells in vitro. *Br J Exp Pathol.* 1982;63:50–55.
32. Rempel D, Abrahamsson SO. The effects of reduced oxygen tension on cell proliferation and matrix synthesis in synovium and tendon explants from the rabbit carpal tunnel: an experimental study in vitro. *J Orthop Res.* 2001;19:143–148.

33. Padilla J, Hamilton SA, Lundgren EA, McKenzie JM, Mickleborough TD. Exercise training in normobaric hypoxia: is carbonic anhydrase III the best marker of hypoxia? *J Appl Physiol.* 2007;103:730–732.
34. Grigsby PW, Malyapa RS, Higashikubo R, et al. Comparison of molecular markers of hypoxia and imaging with ^{60}Cu-ATSM in cancer of the uterine cervix. *Mol Imaging Biol.* 2007;9:278–283.
35. Yuan H, Schroeder T, Bowsher JE, Hedlund LW, Wong T, Dewhirst MW. Intertumoral differences in hypoxia selectivity of the PET imaging agent ^{64}Cu(II)-diacetyl-bis(N^4-methylthiosemicarbazone). *J Nucl Med.* 2006;47:989–998.
36. Laforest R, Dehdashti F, Lewis JS, Schwarz SW. Dosimetry of $^{60/61/62/64}$Cu-ATSM: a hypoxia imaging agent for PET. *Eur J Nucl Med Mol Imaging.* 2005; 32:764–770.
37. Dearling JL, Lewis JS, Mullen GE, Welch MJ, Blower PJ. Copper bis(thiosemicarbazone) complexes as hypoxia imaging agents: structure-activity relationships. *J Biol Inorg Chem.* 2002;7:249–259.
38. Langberg H, Bulow J, Kjaer M. Standardized intermittent static exercise increases peritendinous blood flow in human leg. *Clin Physiol.* 1999;19:89–93.
39. Matsumoto K, Szajek L, Krishna MC, et al. The influence of tumor oxygenation on hypoxia imaging in murine squamous cell carcinoma using [^{64}Cu]Cu-ATSM or [^{18}F]fluoromisonidazole positron emission tomography. *Int J Oncol.* 2007;30: 873–881.
40. Lewis JS, McCarthy DW, McCarthy TJ, Fujibayashi Y, Welch MJ. Evaluation of ^{64}Cu-ATSM in vitro and in vivo in a hypoxic tumor model. *J Nucl Med.* 1999;40:177–183.

Erratum

In the article "PET Imaging of Prostate Cancer Xenografts with a Highly Specific Antibody Against the Prostate-Specific Membrane Antigen," by Elsässer-Beile et al. (*J Nucl Med.* 2009;50:606–611), the image used for Figure 1 was incorrect. The corrected Figure 1 appears below. The authors regret the error.

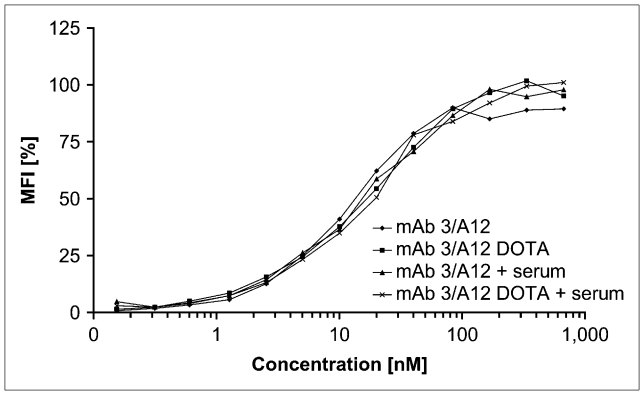

FIGURE 1. Binding of 3/A12 mAb and DOTA-3/A12 mAb, with and without serum preincubation, to PSMA-positive C4-2 cells. Cells were treated with increasing concentrations (0.15–800 nM) of first-step anti-PSMA mAb followed by incubation with saturating amount of second-step phycoerythrin-labeled goat antimouse IgG followed by cytofluorometric analysis. MFI = mean fluorescence intensity.

The Journal of NUCLEAR MEDICINE

Noninvasive ^{64}Cu-ATSM and PET/CT Assessment of Hypoxia in Rat Skeletal Muscles and Tendons During Muscle Contractions

Dorthe Skovgaard, Michael Kjaer, Jacob Madsen and Andreas Kjaer

J Nucl Med. 2009;50:950-958.
Published online: May 14, 2009.
Doi: 10.2967/jnumed.109.062216

The Journal of Nuclear Medicine is published monthly.
SNMMI | Society of Nuclear Medicine and Molecular Imaging
1850 Samuel Morse Drive, Reston, VA 20190.
(Print ISSN: 0161-5505, Online ISSN: 2159-662X)

SNMMI SOCIETY OF NUCLEAR MEDICINE AND MOLECULAR IMAGING